



Involvement of miR-495 overexpression in the pathogenesis of bronchopulmonary dysplasia in preterm infants via the targeting of *NEDD4L-ENaC* pathway

Yi-Fan Sun, Li Ma, Jian-Hui Li, Yuan Yang, Xiao-Hui Gong, Cheng Cai

Department of Neonatology, Shanghai Children's Hospital, School of Medicine, Shanghai Jiao Tong University, Shanghai, China

Contributions: (I) Conception and design: YF Sun, L Ma, C Cai; (II) Administrative support: XH Gong, C Cai; (III) Provision of study materials or patients: All authors; (IV) Collection and assembly of data: All authors; (V) Data analysis and interpretation: YF Sun, L Ma, JH Li, C Cai; (VI) Manuscript writing: All authors; (VII) Final approval of manuscript: All authors.

Correspondence to: Cheng Cai. Department of Neonatology, Shanghai Children's Hospital, School of Medicine, Shanghai Jiao Tong University, No. 355, Luding Road, Shanghai 200062, China. Email: caicheng2004@163.com.

Background: Bronchopulmonary dysplasia (BPD) is a severe pulmonary complication causing morbidity and mortality in preterm infants. A key histopathological feature of BPD is late lung growth retardation, in which the process of alveolarization is hindered and the mechanism of which is unclear. Emerging evidence indicates that microRNAs (miRNAs) promote the development of BPD via the inhibition of their target genes. MiR-495 has been reported to be involved in various lung diseases. However, the physiological function of miR-495 in BPD has not yet been fully understood.

Methods: Differentially expressed miRNAs in peripheral blood of patients with BPD were compared with those of normal controls. A dual-luciferase reporter assay was performed to identify the target genes of miR-495. A BPD neonatal rat model was established by injecting lipopolysaccharide (LPS) in the amniotic sac of pregnant rats. The morphology of the lungs was observed using hematoxylin and eosin (HE) staining. The expression of miR-495, neural precursor cell expressed developmentally down-regulated 4-like (*NEDD4L*), and epithelial Na⁺ channel (*ENaC*) was tested using quantitative reverse transcription-polymerase chain reaction (qRT-PCR), Western blot analysis, and immunofluorescent (IF) staining.

Results: The expression of miR-495 was significantly increased in the peripheral blood samples of premature infants with BPD and verified using qRT-PCR. *NEDD4L* was proven to be the target gene of miR-495. Additionally, miR-495 expression was also increased in the lungs of rat pups with BPD at postnatal day (P) 3 compared with the control group. qRT-PCR and Western blot results showed that *NEDD4L* expression was decreased while *ENaC* expression was increased at the transcriptional and translational levels. IF staining results showed that *NEDD4L* level was decreased while *ENaC* level was increased in the LPS-induced BPD rat model, which was consistent with abnormal changes in alveolar structure.

Conclusions: The aberrant overexpression of miR-495 may contribute to the development of BPD by targeting *NEDD4L-ENaC* pathway, implying an imbalance in lung fluid clearance.

Keywords: MiR-495; bronchopulmonary dysplasia (BPD); neural precursor cell expressed developmentally down-regulated 4-like (*NEDD4L*); epithelial Na⁺ channel (*ENaC*)

Submitted Jun 26, 2022. Accepted for publication Nov 07, 2022. Published online Dec 19, 2022.

doi: 10.21037/atm-22-3293

View this article at: <https://dx.doi.org/10.21037/atm-22-3293>

Introduction

Bronchopulmonary dysplasia (BPD), initially characterized by arrested lung growth, is recognized to emerge as a result of an aberrant reparative response to both antenatal and postnatal injury to the immature lungs of premature infants. Generally, impaired lung development during BPD pathogenesis is attributed to simplified alveolarization and dysmorphic pulmonary vasculature (1,2). To date, BPD remains a major cause of pulmonary diseases in premature newborns, leading to mortality and morbidity despite new advances in treatment (2). An increasing number of studies are finding that the imbalance of lung luminal fluid is involved in the development of BPD through largely unknown mechanisms (1,3). Increased epithelial Na⁺ channel (*ENaC*) activity has been demonstrated to be responsible for alveolar lipid depletion and impaired lung function (4). Thus, better insights into pathobiology will provide a better understanding of BPD and may lead to discoveries of novel therapeutic targets.

Recent studies have shown that noncoding RNAs, especially microRNAs (miRNAs), play an important role in lung development-related diseases. An association of altered expression of multiple miRNAs with impeded alveolarization has been reported (5,6). Increased miR-125b expression has been demonstrated to help protect against BPD, whereas overexpression of miR-184-3p promotes the development of BPD (7,8). MiR-495 has been found to

have multiple regulatory functions in multiple lung diseases, including lung cancer, pulmonary hypertension, acute lung injury, and chronic asthma (9-12). Moreover, miRNA profiling suggests that miR-495 expression is significantly altered at different stages of rat lung development (13). However, there is a lack of data regarding exactly how miR-495 performs its specific function in BPD.

In the present study, we found abnormal overexpression of miR-495 in the peripheral blood of premature infants with BPD. Based on target gene prediction results, the binding ability of miR-495 and 3'-untranslated region (3'UTR) of neural precursor cell expressed developmentally down-regulated 4-like (*NEDD4L*) was confirmed *in vitro*. In a lipopolysaccharide (LPS)-induced BPD neonatal rat model, the suppression of *NEDD4L* led to upregulation of *ENaC*, the key regulator of lung fluid clearance. We hypothesized that aberrant miR-495 overexpression may be involved in BPD by targeting *NEDD4L-ENaC* pathway. We present the following article in accordance with the ARRIVE reporting checklist (available at <https://atm.amegroups.com/article/view/10.21037/atm-22-3293/rc>).

Methods

Participants and sample collection

The peripheral blood samples of 6 premature infants with BPD and 6 age-matched preterm infants without BPD were collected as described in our previous study (14). The time points of peripheral blood sample collection were 28 days after continuous oxygen use in the BPD group and approximately 3 days after birth in the control group. No statistically significant differences were found in the comparisons of general clinical characteristics (postmenstrual age, weight at the time of sample collection, or sex) between the 2 groups (*Table 1*). The study was conducted in accordance with the Declaration of Helsinki (as revised in 2013). The study was approved by the ethics committee of Shanghai Children's Hospital, Shanghai Jiao Tong University (No. 2015RY009-F01), and informed consent was obtained from all the guardians.

Animal model

A total of 12 timed-pregnancy Sprague Dawley (SD) rats were purchased from the Shanghai Laboratory Animal Center (Shanghai, China). The housing conditions met specific pathogen-free (SPF) standards. Pregnant rats were

Highlight box

Key findings

- MiR-495 expression was increased in BPD infants and LPS-induced BPD rat model. *NEDD4L* was proven to be the target gene of miR-495. *NEDD4L* expression was decreased while *ENaC* expression was increased in the LPS-induced BPD rat model, which was consistent with abnormal changes in alveolar structure.

What is known and what is new?

- *ENaC* regulated by *NEDD4L* is a key regulator of fluid balance in lung development. Excessive clearance of alveolar and airway fluid is an important cause of respiratory diseases;
- The aberrant overexpression of miR-495 may contribute to the development of BPD by targeting *NEDD4L-ENaC* pathway, implying an imbalance in lung fluid clearance.

What is the implication, and what should change now?

- Our findings provide a new avenue for exploring the pathogenesis and treatment in BPD. Further experiments on the miR-495-mediated mechanism in BPD are needed.

Table 1 General clinical characteristics of patients in the BPD and control groups

Items	Control group	BPD group	<i>t</i>	P
Postmenstrual age (weeks), mean ± standard error	31.83±0.75	33.54±0.77	-1.60	0.14
Weight (grams), mean ± standard error	1,539.17±32.62	1,729.50±181.63	-1.03	0.35
Sex			-	1 ^a
Female	2	3		
Male	4	3		

^a, Fisher exact test. BPD, bronchopulmonary dysplasia.

randomly allocated to 2 groups, which were exposed to LPS and endotoxin-free saline respectively. LPS (*Escherichia coli* O55:B5) was injected into the amniotic sac as described in our previous study (15). Briefly, LPS (5 µL, 0.2 µg/µL) was injected into the amniotic sac of pregnant rats on embryonic day (E) 16.5. Pregnant rats were injected with sterile endotoxin-free saline (5 µL) as a control. Newborn rats were killed on postnatal day (P) 3. Lungs were stripped from the heart and trachea for further investigation. Animal experiments were performed under a project license (No. 2018009) granted by the ethics committee of Shanghai Children's Hospital, Shanghai Jiao Tong University, in compliance with its guidelines for the care and use of animals.

Dual-luciferase reporter assay

The information of binding sites between miR-495 and target genes was obtained by DIANA MicroT-CDS (University of Thessaly, Volos, Greece). A549 cells were seeded in 96-well plates and incubated for 24 hours to reach 60% to 70% confluency. *NEDD4L* 3'UTR and *NEDD4L* 3'UTR mutant (Mut) reporter plasmids were constructed in advance. A549 cells were transiently co-transfected with miR-495 mimics or miR-495 inhibitors together with 0.2 µg of pmiR-negative control (NC), pmiR-*NEDD4L*-3'UTR-wild type (WT), or pmiR-*NEDD4L*-3'UTR-Mut reporter plasmids using Lipofectamine 2000 (Thermo Fisher Scientific, Waltham, MA, USA) according to the manufacturer's instruction. After 24 hours of incubation, firefly and renilla luciferase activities were detected using a Dual-Luciferase Reporter Assay System (CAS: E2920; Promega, Madison, WI, USA) and recorded employing a SpectraMax M5 (Molecular Devices, San Jose, CA, USA).

Hematoxylin and eosin (HE) staining

Lung tissue was insufflated, fixed with 4% buffered

paraformaldehyde, dehydrated, and then embedded in paraffin. Sections were dewaxed with xylene at 3-4 µm thickness and hydrated in ethanol-water solutions of different concentration gradients. The sections were then stained with hematoxylin for 5 minutes, differentiated with 1% ethanol hydrochloride for 3 seconds, and transferred to an eosin solution for 2 minutes. Finally, they were dehydrated and mounted. PANNORAMIC scan (3DHISTECH, Budapest, Hungary) and CaseViewer (3DHISTECH) were used for analysis.

Immunofluorescent (IF) staining

Paraffin sections of lung tissue were used for IF staining. These sections were incubated with the primary antibody for 24 hours at 4 °C and then washed 3 times (5 minutes each) with phosphate-buffered saline (PBS). Primary antibodies against NEDD4L (ab46521; 1:200; Abcam, Cambridge, UK) and ENaC-α (ab214192; 1:200; Abcam) were used in this study. Then, these sections were incubated for 50 minutes at room temperature in the dark with horseradish peroxidase (HRP)-conjugated goat anti-rabbit secondary antibody (GB25303;1:400; Servicebio, Wuhan, China) and nuclei-stained with 4',6-diamidino-2-phenylindole (DAPI; Beyotime, Jiangsu, China). The images were captured using confocal fluorescence microscopy (Nikon, Tokyo, Japan). All immunostaining images are representative of at least 3 independent biological experiments.

RNA extraction and quantitative reverse transcription-polymerase chain reaction (qRT-PCR)

TRIzol reagent (Thermo Fisher Scientific) was used for the extraction of RNA, and a NanoDrop 2000 Spectrophotometer (Thermo Fisher Scientific) was employed for the control and detection of RNA quantity. First-strand complement (cDNA) was generated using

Table 2 Primers for reverse transcription

Variables	Sequence (5'-3')
hsa-miR-495	GTCGTATCCAGTGCCTGTCGTGGAGTCGG CAATTGCACTGGATACGACCGAAAA
U6	CGCTTCACGAATTTGCGTGTCA

Table 3 Primers for polymerase chain reaction

Variables	Sequence (5'-3')
hsa-miR-495	F: GGGGAAGTTGCCCATGTTA R: GTGCGTGTCTGGAGTCG
U6	F: GCTTCGGCAGCACATACTAAAT R: CGCTTCACGAATTTGCGTGTCA

a miRNA 1st Strand cDNA Synthesis Kit (Vazyme, Jiangsu, China). RNA samples were subjected to reverse transcription with a Reverse Transcription Kit (Abclonal, Wuhan, China) and real-time PCR with SYBR Green (Abclonal). PCR was carried out with an ABI 7500 thermal cycler (Applied Biosystems, Thermo Fisher Scientific) using the following 2-step cycling program: 95 °C for 3 minutes, 40 cycles at 95 °C for 5 seconds, and 60 °C for 34 seconds. Dissociation curves were generated for both genes based on the default. The expression levels of the miR-495 genes were normalized to that of an internal control, U6, to obtain relative threshold cycle (ΔC_t) values. Relative quantification of gene expression was achieved by normalization against an endogenous control, glyceraldehyde-3-phosphate dehydrogenase (*GAPDH*). The $2^{-\Delta\Delta C_t}$ method was used for the comparison of relative expression levels (13). The specific primers for RNA samples of peripheral blood are shown in *Tables 2,3*. The specific primers of miR-495 and U6 for rat lung RNA samples were obtained from RiboBio (R10031.7; Guangzhou, China). *ENaC- α* (RP301306; Sino Biological, Beijing, China), *NEDD4L* (RP301305), and *GAPDH* (RP300644; Sino Biological) were also used in the process.

Protein extraction and Western blot analysis

Radioimmunoprecipitation assay buffer (Beyotime Institute of Biotechnology) was used for the extraction of proteins, and the bicinchoninic acid (BCA) method (Beyotime Institute of Biotechnology) was used for the measurement

of concentrations. Proteins (40 μ g/lane) were loaded on 8% sodium dodecyl-sulfate polyacrylamide gel electrophoresis (SDS-PAGE) gels and transferred onto a polyvinylidene fluoride (PVDF) membrane (EMD Millipore, Billerica, MA, USA). The membrane was blocked for nonspecific binding for 2 hours by incubation with 5% fat-free dry milk in 100 mM of Tris-buffered saline plus 0.1% Tween-18 (TBST). Primary antibodies included rabbit anti-NEDD4L antibody (ab46521; 1:1,000; Abcam), rabbit anti-ENaC- α antibody (ab214192; 1:1,000; Abcam), and rabbit anti-GAPDH antibody (KGAA002; 1:1,000; Nanjing KeyGen Biotech Co., Ltd., Nanjing, China). The membrane was incubated with primary antibodies overnight at 4 °C and then washed with TBST 3 times. The membrane was then incubated with HRP-conjugated goat-anti-rabbit secondary antibody (bs-0295G-HRP; 1:2,000; Bioss, Woburn, MA, USA) for 1.5 hours at room temperature. The enhanced chemiluminescence detection system (ChemiDoc XRS + Imaging System; Bio-Rad Laboratories, Inc., Hercules, CA, USA) was used to visualize the bands of antibody-detected proteins.

Statistical analysis

The results are presented as the mean \pm standard error. All experiments were repeated 3 times. Chi-square tests and Student's *t*-tests were used to analyze significant differences with the SPSS 22.0 software (IBM Corp., Armonk, NY, USA). $P < 0.05$ was considered to indicate statistical significance.

Results

MiR-495 expression increased in the peripheral blood of premature infants with BPD

In a previous study, we compared and analyzed the differentially expressed miRNAs in peripheral blood of premature infants with BPD using microarray expression profiling, and the results have been submitted to the Gene Expression Omnibus (GEO) database (GSE108755; National Center for Biotechnology Information, National Institutes to Health, Bethesda, MD, USA) (14). To date, various miRNAs have been found to be differentially expressed, as shown in *Figure 1A*. To our knowledge, miR-495 has been reported as being involved in regulating lung development and various lung diseases by targeting a series of downstream signaling pathways (9-13). To investigate the

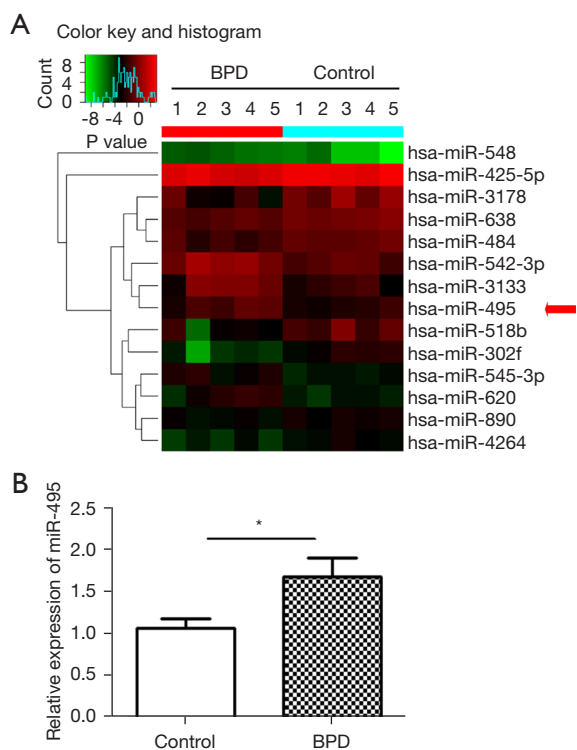


Figure 1 Altered miR-495 expression in neonates with BPD. (A) A number of miRNAs were differentially expressed in the BPD and control groups. Some are shown in this figure. (B) The result of qRT-PCR showed that the miR-495 expression was significantly increased in the peripheral blood of the BPD group compared with the control group (n=6; *, P<0.05). BPD, bronchopulmonary dysplasia; miRNA, microRNA; qRT-PCR, quantitative reverse transcription-polymerase chain reaction.

role of miR-495 in BPD, we reanalyzed miR-495 expression in the peripheral blood samples of 6 premature infants with BPD and 6 age-matched preterm infants without BPD with qRT-PCR. In accordance with the array findings, the expression of miR-495 was significantly increased in the BPD group compared with the control group (Figure 1B).

MiR-495 directly targeted NEDD4L by interacting with the 3'UTR in A549 cells

We explored the potential mechanism of the regulatory effect of miR-495 by using the bioinformatic prediction of DIANA MicroT-CDS. We obtained the binding site for *NEDD4L* to miR-495. As shown in Figure 2A, the miR-495 seed sequence possesses a nucleotide sequence complementary to the 3'UTR region of *NEDD4L* (P=0.006).

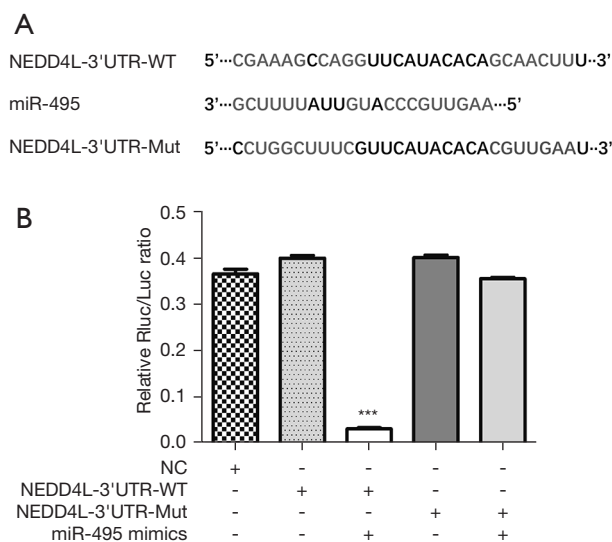


Figure 2 miR-495 directly targeted *NEDD4L* by interaction with the 3'UTR. (A) Binding sites of miR-495 and *NEDD4L*. (B) Analysis of the luciferase activity of *NEDD4L* 3'UTR WT and MUT vectors in A549 cells using miR-495. The result shows that miR-495 downregulated the expression of *NEDD4L* (n=3; ***, P<0.001). *NEDD4L*, neural precursor cell expressed developmentally down-regulated 4-like; 3'UTR, 3' untranslated region; MUT, mutant; WT, wild type; Rluc/Luc, renilla luciferase/luciferase.

For further confirmation, dual-luciferase reporter assay was used based on the predicted binding sites of miR-495 and *NEDD4L*. The results revealed that miR-495 in A549 cells negatively regulated the luciferase activity of the 3'UTR region of *NEDD4L*. In addition, miR-495 had no regulatory effect on *NEDD4L* when the predicted binding sites were mutated (Figure 2B). The above results indicate that *NEDD4L* was the direct target gene of miR-495.

Intra-amniotic LPS injection disrupted alveolar development in newborn rats

As the lung development and sequences of miRNAs are well conserved in humans and rats, we established a rat model of BPD for further studying miR-495 regulatory downstream signaling *in vivo*. LPS dissolved in saline or saline only was injected into the amniotic sac of pregnant rats at E16.5. All animals survived. The newborn rats were lactated until being killed at P3. HE staining was performed for morphological observation of lung tissues. Lung tissues of the LPS-treated rats showed a simplified alveolar structure compared with

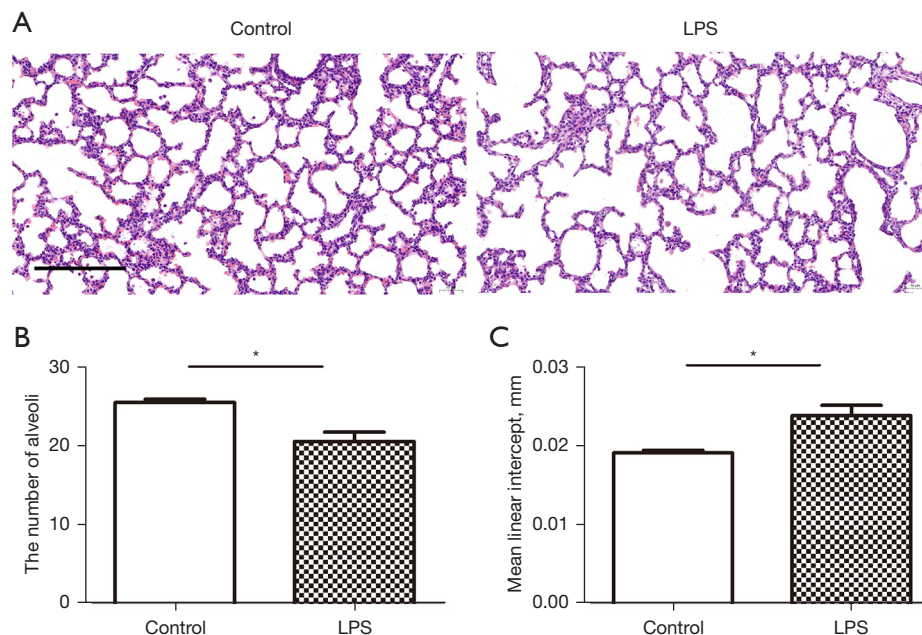


Figure 3 Simplified alveolar structure of LPS-treated rat lungs. (A) Pregnant rats were injected with LPS or saline at E16.5. HE staining was used to analyze the lung morphometry of newborns at P3. A simplified alveolar structure was observed in the lungs of the LPS-treated group compared with the control group (magnification, 20 \times). (B) Compared with the control group, fewer alveoli were detected in the lungs of LPS-treated groups at P3 (n=3; * P<0.05). (C) At P3, rats of the LPS-treated groups had a significantly greater MLI than did rats of the control groups (n=3; * P<0.05). LPS, lipopolysaccharide; E, embryonic day; HE, hematoxylin and eosin; P, postnatal day; MLI, mean linear intercept.

the control group (Figure 3A). The lungs of the LPS-treated group showed significantly fewer alveoli and greater mean linear intercept (MLI) at P3 (Figure 3B,3C) compared with the control group. These findings suggest that the alveolar development of newborn rats was disrupted by intraamniotic LPS injection mimicking BPD.

MiR-495, NEDD4L, and ENaC expression altered in the BPD rat model

As mentioned above, *NEDD4L* is a target gene of miR-495. Previous studies have shown that *NEDD4L* overexpression inhibits the activation of *ENaC*, which is a key regulator of fluid balance in lung development and is involved in the transition from lung fluid secretion to fluid absorption (16,17). Therefore, qRT-PCR, Western blot, and IF were performed to detect the expression of miR-495, *NEDD4L*, and *ENaC* in rat lungs with BPD. As shown in Figure 4A, the miR-495 expression of rat lungs in the LPS-treated group at P3 was significantly increased compared with rat lungs in the control group. The qRT-PCR analyses also

showed a significant decrease in *NEDD4L* expression and an increase in *ENaC* expression in the LPS-treated lungs at P3 (Figure 4A). The results of the Western blot showed that *NEDD4L* level in the LPS-treated group was reduced compared with that in the control group (Figure 4B). The *ENaC* level, which was negatively regulated by *NEDD4L*, was increased in the LPS-treated group (Figure 4C). Likewise, the results of IF revealed the decreased level of *NEDD4L* and the increased level of *ENaC* in LPS-treated lungs (Figure 5). These findings support the hypothesis that miR-495 has important role in the pathogenesis of BPD via the targeting of *NEDD4L-ENaC* pathway.

Discussion

In the present study, we found that miR-495 overexpression was involved in arrested lung development of BPD via regulation of *NEDD4L-ENaC* pathway. The overexpression of miR-495 inhibited the expression of *NEDD4L*, which resulted in the overexpression of *ENaC*. *ENaC* has been reported to be a key regulator of fluid balance in lung

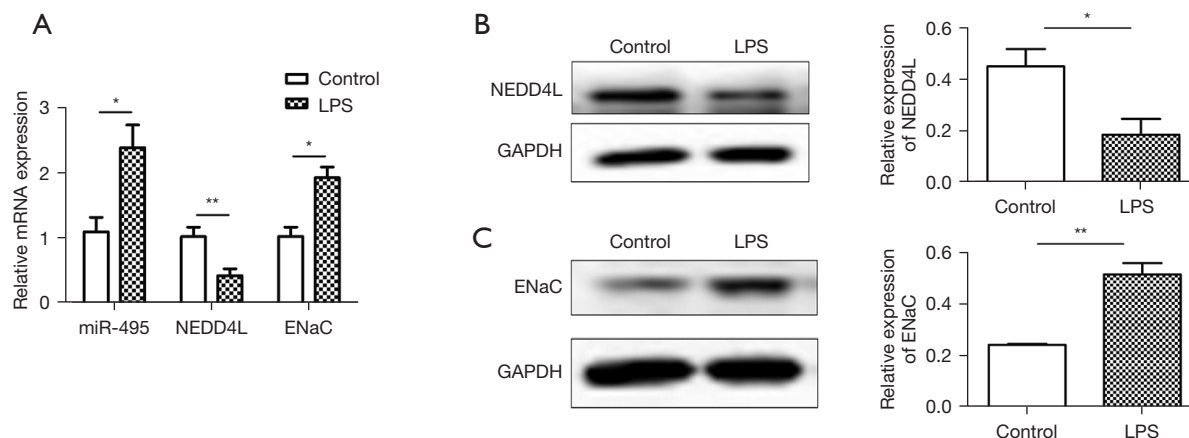


Figure 4 The expression of miR-495, *NEDD4L*, and *ENaC* in the BPD rat model. (A) The expression of miR-495 and *ENaC* was significantly increased in rat lungs of the LPS-treated groups versus the control group at P3. Decreased expression of *NEDD4L* in LPS-treated rat lungs was also detected (n=6; *, P<0.05; **, P<0.01). (B,C) Gene expression at the protein level was examined using Western blot. Compared with the control rats at P3, the level of *NEDD4L* was decreased and the level of *ENaC- α* was increased in the LPS-treated rats (n=3; *, P<0.05; **, P<0.01). *NEDD4L*, neural precursor cell expressed developmentally down-regulated 4-like; *ENaC*, epithelial Na⁺ channel; LPS, lipopolysaccharide; GAPDH, glyceraldehyde-3-phosphate dehydrogenase; BPD, bronchopulmonary dysplasia; P, postnatal day.

development (16,17). The findings suggest that miR-495 might be a potential therapeutic target for BPD.

Notably, miRNAs have been increasingly recognized as playing important roles in lung development and related diseases (18). In our previous study, several miRNAs, including miR-495, were found to be dysregulated in premature infants with BPD compared with normal infants (14). Yang and colleagues found that miR-495 expression underwent significantly dynamic changes in rat lung development. The expression of miR-495 was upregulated from canalicular to saccular stages and downregulated from saccular to alveolar stages (13). The above findings suggest that the altered expression of miR-495 might participate in the regulation of lung development in BPD. We also detected increased expression of miR-495 in the peripheral blood of infants with BPD using qRT-PCR, which was opposite to the findings in normal rat lung development. Therefore, miR-495 was considered to serve an important role in lung development and BPD.

Identification of target genes is important for researchers to further study the role of miR-495 in BPD. *NEDD4L* (also known as *NEDD4-2*) is a ubiquitin-protein ligase in the *NEDD4L* family that can regulate a number of membrane proteins and that figures prominently in the maintenance of homeostasis in cells (19). *NEDD4L* is highly conserved in vertebrates and extensively expressed in the liver, kidney, heart, and lung. Moreover, it has been reported to be

involved in the secretion of the lung surfactant protein C (*SP-C*), but its major function is to regulate the stability of *ENaC* in the kidney, lung, and other organs (20-22). In our study, the luciferase reporter assay showed that miR-495 suppressed the expression of *NEDD4L* through 3'UTR binding. Based on the above findings, we concluded that miR-495 negatively regulated *NEDD4L*, and both miR-495 and *NEDD4L* were involved in BPD.

The successful establishment of an animal model of BPD was important for further study of miR-495 mechanisms *in vivo*. The pathognomonic characteristics of BPD are impaired alveolarization and dysregulated vascularization (1,2). Previous studies have shown that intra-amniotic injection of LPS into pregnant SD rats at E16.5 results in phenotypes similar to BPD (15,23). Consistent with previous studies, intra-amniotic injection of LPS into SD rats at E16.5 in our study resulted in fewer and simplified alveoli compared with the control group, which serves as an ideal animal model with pathological characteristics of BPD (15,23).

By using the BPD rat model, qRT-PCR, Western blot, and IF were carried out for further investigation. As mentioned above, the main function of *NEDD4L*, which was targeted by miR-495, was to regulate the expression of *ENaC*. *ENaC* has been reported to be highly expressed in both airway epithelial cells and type II alveolar cells (AECIIs) and to be responsible for lung fluid balance, which is important for neonates for

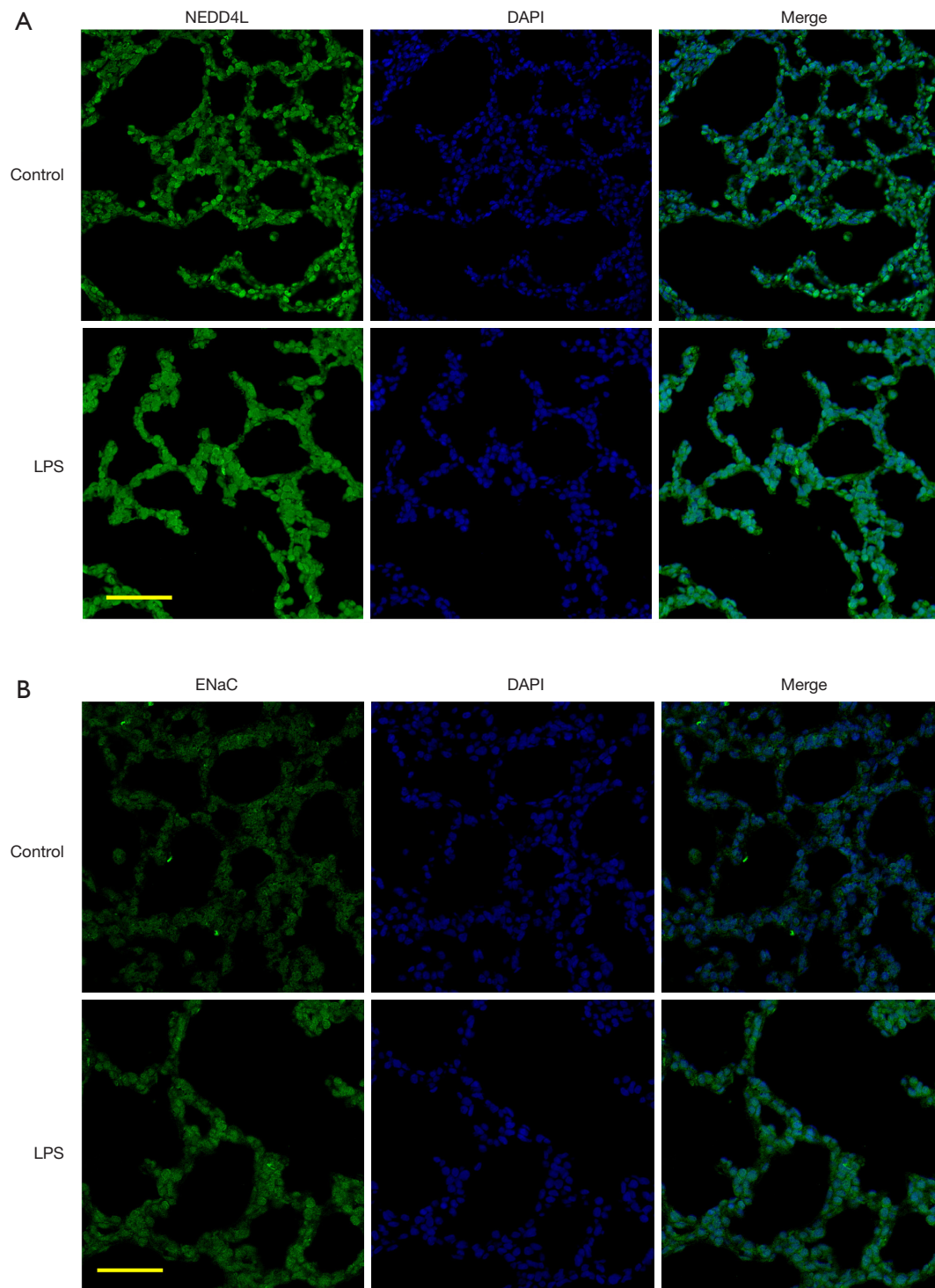


Figure 5 Expression of NEDD4L and ENaC in the BPD rat model detected by IF. (A,B) Differentiated lung tissues were treated with indicated agent's immunoassayed with DAPI (blue), anti-ENaC- α (green) and anti-NEDD4L (green). Observation under an inverted fluorescence microscope at 40 \times . The results showed that NEDD4L level was decreased while ENaC- α level was increased in the LPS-treated group versus control groups (n=3). NEDD4L, neural precursor cell expressed developmentally down-regulated 4-like; ENaC, epithelial Na⁺ channel; BPD, bronchopulmonary dysplasia; IF, immunofluorescence; LPS, lipopolysaccharide.

establishing effective spontaneous breathing after birth (17,20,24). Previous studies have shown that excessive lung fluid caused by decreasing levels and activity of *ENaC* contributes to various respiratory diseases (25-27). Notably, a growing number of studies in recent years have shown that excessive clearance of lung fluid regulated by the *NEDD4L-ENaC* pathway is also an important cause of dyspnea (28-30). In one study, the airway-specific overexpression of *ENaC* of mice exhibited airway surface dehydration and impaired mucociliary clearance and provided a nidus for bacterial infection, which led to a model of lung disease that shares key features of chronic obstructive pulmonary diseases (24). Deletion of *NEDD4L* in lung epithelial cells enhances the fluid clearance function of *ENaC* and leads to accumulation of airway mucus, neutrophils, and other inflammatory factors (28-31). Moreover, it has been reported that neutrophils in the alveoli secrete pathogenic exosomes. These exosomes result in impaired and simplified alveolar structure, increased airway resistance, and other pathological changes characteristic of a BPD-like phenotype (32). The study by Boase and colleagues showed similar findings in *NEDD4L*-deficient mice (29). In our study, the expression of miR-495 was increased in BPD rat lungs, *NEDD4L* was downregulated, and *ENaC* was up-regulated at both the mRNA and protein levels in BPD rat models. In summary, it can be concluded that miR-495 might affect the lung fluid balance to promote BPD via the *NEDD4L-ENaC* pathway.

Although the present study explored the potential role of miR-495 in BPD, it has some limitations. The process of lung development is continuous, and the lungs of premature infants after birth are still at the middle or late development stages. In our study, there was a lack of dynamic observation of the relationship between miR-495 and lung development during BPD. Moreover, our findings suggested that miR-495 targeted *NEDD4L-ENaC* pathway and might regulate the balance of lung fluid in BPD, but the molecular mechanism still needs further investigation *in vitro* and *in vivo*. Further experiments on inhibiting miR-495 overexpression *in vivo* need to be performed to confirm the miR-495-mediated mechanism in BPD.

Conclusions

In conclusion, the findings of the present study suggest that miR-495 serves an essential role in BPD. Moreover, miR-495 activates the *NEDD4L-ENaC* pathway by inhibiting the expression of *NEDD4L*, resulting in overexpression of *ENaC*, which has been reported to be important in

the clearance of lung fluid. These results may provide a potential and promising direction for BPD treatment. Our findings provide a new avenue for exploring the pathogenesis and treatment in BPD.

Acknowledgments

Funding: This research was funded by the National Natural Science Foundation of China 10.13039/501100001809 (grant No. 81801489 to JH Li).

Footnote

Reporting Checklist: The authors have completed the ARRIVE reporting checklist. Available at <https://atm.amegroups.com/article/view/10.21037/atm-22-3293/rc>

Data Sharing Statement: Available at <https://atm.amegroups.com/article/view/10.21037/atm-22-3293/dss>

Peer Review File: Available at <https://atm.amegroups.com/article/view/10.21037/atm-22-3293/prf>

Conflicts of Interest: All authors have completed the ICMJE uniform disclosure form (available at <https://atm.amegroups.com/article/view/10.21037/atm-22-3293/coif>). The authors have no conflicts of interest to declare.

Ethical Statement: The authors are accountable for all aspects of the work in ensuring that questions related to the accuracy or integrity of any part of the work are appropriately investigated and resolved. The study was conducted in accordance with the Declaration of Helsinki (as revised in 2013) and was approved by the ethics committee of Shanghai Children's Hospital, Shanghai Jiao Tong University (No. 2015RY009-F01). Informed consent was obtained from all the guardians. Animal experiments were performed under a project license (No. 2018009) granted by the ethics committee of Shanghai Children's Hospital, Shanghai Jiao Tong University, in compliance with its guidelines for the care and use of animals.

Open Access Statement: This is an Open Access article distributed in accordance with the Creative Commons Attribution-NonCommercial-NoDerivs 4.0 International License (CC BY-NC-ND 4.0), which permits the non-commercial replication and distribution of the article with the strict proviso that no changes or edits are made and the

original work is properly cited (including links to both the formal publication through the relevant DOI and the license). See: <https://creativecommons.org/licenses/by-nc-nd/4.0/>.

References

1. Thébaud B, Goss KN, Laughon M, et al. Bronchopulmonary dysplasia. *Nat Rev Dis Primers* 2019;5:78.
2. Sahni M, Bhandari V. Recent advances in understanding and management of bronchopulmonary dysplasia. *F1000Res* 2020;9:eF1000 Faculty Rev-703.
3. Cotten CM. Pulmonary hypoplasia. *Semin Fetal Neonatal Med* 2017;22:250-5.
4. Livraghi-Butrico A, Wilkinson KJ, Volmer AS, et al. Lung disease phenotypes caused by overexpression of combinations of α -, β -, and γ -subunits of the epithelial sodium channel in mouse airways. *Am J Physiol Lung Cell Mol Physiol* 2018;314:L318-31.
5. Das P, Shah D, Bhandari V. miR34a: a novel small molecule regulator with a big role in bronchopulmonary dysplasia. *Am J Physiol Lung Cell Mol Physiol* 2021;321:L228-35.
6. Dravet-Gounot P, Morin C, Jacques S, et al. Lung microRNA deregulation associated with impaired alveolarization in rats after intrauterine growth restriction. *PLoS One* 2017;12:e0190445.
7. Zhang X, Chu X, Gong X, et al. The expression of miR-125b in Nrf2-silenced A549 cells exposed to hyperoxia and its relationship with apoptosis. *J Cell Mol Med* 2020;24:965-72.
8. Retraction notice for: "miR-184 mediates hyperoxia-induced injury by targeting cell death and angiogenesis signalling pathways in the developing lung." Dilip Shah, Karmyodh Sandhu, Pragnya Das, Zubair H. Aghai, Sture Andersson, Gloria Pryhuber and Vineet Bhandari. *Eur Respir J* 2020; in press. *Eur Respir J* 2021;58:1901789.
9. Sun J, Qiao Y, Song T, et al. MiR-495 suppresses cell proliferation by directly targeting HMGA2 in lung cancer. *Mol Med Rep* 2019;19:1463-70.
10. Fu J, Bai P, Chen Y, et al. Inhibition of miR-495 Improves Both Vascular Remodeling and Angiogenesis in Pulmonary Hypertension. *J Vasc Res* 2019;56:97-106.
11. Ying Y, Mao Y, Yao M. NLRP3 Inflammasome Activation by MicroRNA-495 Promoter Methylation May Contribute to the Progression of Acute Lung Injury. *Mol Ther Nucleic Acids* 2019;18:801-14.
12. Collison A, Herbert C, Siegle JS, et al. Altered expression of microRNA in the airway wall in chronic asthma: miR-126 as a potential therapeutic target. *BMC Pulm Med* 2011;11:29.
13. Yang Y, Pu XD, Qing K, et al. Identification of differentially expressed microRNAs and the possible role of miRNA-126* in Sprague-Dawley rats during fetal lung development. *Mol Med Rep* 2013;7:65-72.
14. Gong X, Qiu J, Qiu G, et al. Adrenomedullin regulated by miRNA-574-3p protects premature infants with bronchopulmonary dysplasia. *Biosci Rep* 2020;40:BSR20191879.
15. Li J, Li Y, He H, et al. Csk/Src/EGFR signaling regulates migration of myofibroblasts and alveolarization. *Am J Physiol Lung Cell Mol Physiol* 2016;310:L562-71.
16. Henshall TL, Manning JA, Alfassy OS, et al. Deletion of Nedd4-2 results in progressive kidney disease in mice. *Cell Death Differ* 2017;24:2150-60.
17. Li T, Koshy S, Folkesson HG. Involvement of {alpha} ENaC and Nedd4-2 in the conversion from lung fluid secretion to fluid absorption at birth in the rat as assayed by RNA interference analysis. *Am J Physiol Lung Cell Mol Physiol* 2007;293:L1069-78.
18. Sun YF, Kan Q, Yang Y, et al. Knockout of microRNA-26a promotes lung development and pulmonary surfactant synthesis. *Mol Med Rep* 2018;17:5988-95.
19. Manning JA, Kumar S. Physiological Functions of Nedd4-2: Lessons from Knockout Mouse Models. *Trends Biochem Sci* 2018;43:635-47.
20. Conkright JJ, Apsley KS, Martin EP, et al. Nedd4-2-mediated ubiquitination facilitates processing of surfactant protein-C. *Am J Respir Cell Mol Biol* 2010;42:181-9.
21. Goel P, Manning JA, Kumar S. NEDD4-2 (NEDD4L): the ubiquitin ligase for multiple membrane proteins. *Gene* 2015;557:1-10.
22. Jiang C, Kawabe H, Rotin D. The Ubiquitin Ligase Nedd4L Regulates the Na/K/2Cl Co-transporter NKCC1/SLC12A2 in the Colon. *J Biol Chem* 2017;292:3137-45.
23. Li H, Yuan X, Tang J, et al. Lipopolysaccharide disrupts the directional persistence of alveolar myofibroblast migration through EGF receptor. *Am J Physiol Lung Cell Mol Physiol* 2012;302:L569-79.
24. Zhou-Suckow Z, Duerr J, Hagner M, et al. Airway mucus, inflammation and remodeling: emerging links in the pathogenesis of chronic lung diseases. *Cell Tissue Res* 2017;367:537-50.
25. Londino JD, Lazrak A, Collawn JF, et al. Influenza virus infection alters ion channel function of airway and alveolar

- cells: mechanisms and physiological sequelae. *Am J Physiol Lung Cell Mol Physiol* 2017;313:L845-58.
26. He J, Qi D, Tang XM, et al. Rosiglitazone promotes ENaC-mediated alveolar fluid clearance in acute lung injury through the PPAR γ /SGK1 signaling pathway. *Cell Mol Biol Lett* 2019;24:35.
27. Aggarwal S, Lazrak A, Ahmad I, et al. Reactive species generated by heme impair alveolar epithelial sodium channel function in acute respiratory distress syndrome. *Redox Biol* 2020;36:101592.
28. Kimura T, Kawabe H, Jiang C, et al. Deletion of the ubiquitin ligase Nedd4L in lung epithelia causes cystic fibrosis-like disease. *Proc Natl Acad Sci U S A* 2011;108:3216-21.
29. Boase NA, Rychkov GY, Townley SL, et al. Respiratory distress and perinatal lethality in Nedd4-2-deficient mice. *Nat Commun* 2011;2:287.
30. Scoville DK, Botta D, Galdanes K, et al. Genetic determinants of susceptibility to silver nanoparticle-induced acute lung inflammation in mice. *FASEB J* 2017;31:4600-11.
31. Duerr J, Leitz DHW, Szczygiel M, et al. Conditional deletion of Nedd4-2 in lung epithelial cells causes progressive pulmonary fibrosis in adult mice. *Nat Commun* 2020;11:2012.
32. Genschmer KR, Russell DW, Lal C, et al. Activated PMN Exosomes: Pathogenic Entities Causing Matrix Destruction and Disease in the Lung. *Cell* 2019;176:113-126.e15.

Cite this article as: Sun YF, Ma L, Li JH, Yang Y, Gong XH, Cai C. Involvement of miR-495 overexpression in the pathogenesis of bronchopulmonary dysplasia in preterm infants via the targeting of *NEDD4L-ENaC* pathway. *Ann Transl Med* 2023;11(1):4. doi: 10.21037/atm-22-3293